

# The Asymmetric Exclusion Process Revisited: Fluctuations and Dynamics in the Domain Wall Picture

Ludger Santen<sup>1</sup> and Cécile Appert<sup>1</sup>

*Received March 13, 2001; accepted July 27, 2001*

---

We investigate the total asymmetric exclusion process by analyzing the dynamics of the shock. Within this approach we are able to calculate the fluctuations of the number of particles and density profiles not only in the stationary state but also in the transient regime. We find that the analytical predictions and the simulation results are in excellent agreement.

---

**KEY WORDS:** Asymmetric exclusion process; boundary induced phase transitions; domain wall theory; transient regime.

## 1. INTRODUCTION

The total asymmetric exclusion process (TASEP) is maybe the most simple lattice model of collective particle transport.<sup>(1–3)</sup> It can be interpreted, e.g., as a basic model of traffic flow<sup>(4)</sup> or as a model for biological transport.<sup>(5)</sup> In generic steady states, these processes are characterized by a non-vanishing mass transport which leads to an intrinsic non-equilibrium behavior. This is interesting from a theoretical point of view. For example, the stationary probabilities of the system are not given by an equilibrium ensemble. Of particular interest are systems with open boundary conditions because one can observe transitions between different bulk states induced by tuning the boundary conditions.<sup>(6)</sup>

Another reason for the importance of the TASEP model is the possibility to find an exact solution for the stationary state. This has been done by solving recursion relations for the stationary partition function.<sup>(7–10)</sup>

---

<sup>1</sup>Laboratoire de Physique Statistique (Laboratoire associé aux universités Paris 6, Paris 7 et au CNRS), École Normale Supérieure, 24 rue Lhomond, F-75231 Paris Cedex 05, France; e-mail: appert@lps.ens.fr and santen@lusi.uni-sb.de

Later a phenomenological approach, referred to as domain wall (DW) theory, was proposed<sup>(11)</sup> which was able to reproduce the exact results for the phase diagram, in the limit of large system sizes.<sup>(12)</sup> The interest of the latter theory is twofold: First, it leads to an intuitive understanding of the most important features of the system and second it can be generalized to more complicated models which are out of scope for an exact treatment.<sup>(13, 14)</sup>

In our article we test the accuracy of the DW theory for the TASEP on finite open lattices. In particular we compare the stationary fluctuations of the number of particles, which are related to the integrated two-point correlation functions. Beyond that we also analyze the non-stationary behavior of TASEP, which cannot be treated with exact methods. Rather than investigating the relaxation spectrum of the process,<sup>(15)</sup> for which numerical evaluation is limited to very small system sizes ( $L \leq 10$ ), we focus on the dynamics of directly observable quantities. We calculated, e.g., the time dependent density profiles, which can be compared easily to simulations (which can be easily carried out on much larger system sizes).

The outline of this paper is as follows. In Section 2 we give a definition of the model and remind briefly of the most important features of the DW theory. Then we compare the predictions for the fluctuations of the number of particles with simulation results. Finally (Section 4), we show how the system responds to a change of boundary conditions.

## 2. THE TASEP WITH OPEN BOUNDARIES

### 2.1. Definition of the Model

The TASEP is defined on a one-dimensional lattice of length  $L$ . Each lattice site ( $i$ ) can be occupied by one particle ( $\tau_i = 1$ ) or be empty ( $\tau_i = 0$ ). In continuous time the dynamics of the particles is defined as follows: A pair of sites ( $i, i+1$ ) is chosen with probability  $dt$ , where  $dt$  denotes an infinitesimal time-step. If the site ( $i$ ) is occupied and the site ( $i+1$ ) is empty one exchanges the positions of particle and hole. All other local configurations are unchanged. In case of open boundary conditions one additionally has to define the in- and output of particles. At a given time a particle can be introduced on the first site with probability  $\alpha dt$  if the first site is empty. If the last site of the chain is occupied the particle may escape from the chain with probability  $\beta dt$ .

The TASEP with continuous time dynamics can be implemented by a random sequential update, i.e., one first chooses randomly a link between two sites and then performs the local update. A possible implementation of the open boundaries is to add two additional sites  $0, L+1$  to the chain,

which are occupied with probability  $\alpha$  and  $1 - \beta$  respectively, and act as particle reservoirs. By definition, one time step includes  $L + 1$  link choices, and the corresponding local updates.

For the TASEP it has been shown that the partition function, i.e., the sum of all stationary weights for a system of size  $L + 1$ , can be obtained recursively from the results for a system of size  $L$ .<sup>(7,8)</sup> The recursion relations have been solved exactly,<sup>(9)</sup> e.g., by means of a matrix representation (MPA).<sup>(10)</sup> Now we shall discuss how most of these results can be recovered using the DW theory.

## 2.2. Domain Wall Theory

The domain wall (DW) theory<sup>(11)</sup> gives a phenomenological description of the system dynamics. The basic idea of this picture is that, as long as the entrance (exit) capacity does not exceed the capacity of the chain, each particle reservoir enforces a domain (of constant density) in the bulk. At a given time both domains coexist in the chain. The coexistence of two domains in the chain implies the existence of a shock, i.e., a region where the two domains meet. In the domain wall theory one assumes that the shock is sharp, i.e., that it has a finite width  $W$ . For a large class of driven lattice gases this requirement is fulfilled and one has  $W \ll L$  already for moderate system sizes  $L$ . After the introduction of the DW theory for the TASEP it has also been successfully applied to models discrete in time and without particle hole symmetry.<sup>(14,18)</sup> Therefore the DW theory provides a quite general theoretical framework for models of particle transport.

Below we now cite the ingredients of the DW theory which are of relevance for the remaining part of the article. In this theoretical frame, the dynamics of the shock determines the behavior of the system. A first characterization of the shock dynamics is possible by means of the lattice continuity equation

$$\frac{d}{dt} \rho(i, t) = j_{i-1}(t) - j_i(t), \quad (1)$$

where  $j_i(t)$  denotes the local particle current at position  $i$  and time  $t$  and  $\rho(i, t)$  the density at the same site. By evaluating this in the continuum limit for the shock position one finds that the shock moves far from the boundaries with velocity

$$V = \frac{j_+ - j_-}{\rho_+ - \rho_-}, \quad (2)$$

where  $\rho_+(\rho_-)$  and  $j_+(j_-)$  are respectively the densities and fluxes in the right (left) domains separated by the shock.

The motion of the domain wall can be interpreted as a random walk with hopping rates

$$D_+ = \frac{j_+}{(\rho_+ - \rho_-)}, \quad D_- = \frac{j_-}{(\rho_+ - \rho_-)} \quad (3)$$

for a move to the right (left).<sup>(11)</sup> In case of a blocked entrance or exit one can easily verify that the dynamics of the domain wall is described correctly. In order to generalize this observation, one uses that both particle reservoirs are independent. The interpretation of the shock dynamics as a random walk allows for an easy calculation of several quantities of interest.

Now we specify the above quantities for the TASEP. An input rate  $\alpha$  leads to a bulk density  $\rho_- = \alpha$  and an output rate  $\beta$  to  $\rho_+ = 1 - \beta$ . Inside each domain one obtains the same behavior as for the periodic system, e.g., one gets  $j = \rho(1 - \rho)$  for the flow.

In case of the TASEP one obtains still good results if one assumes that one can identify a single link as the position of the shock. The link is labeled  $i$  if localized between sites  $i$  and  $i + 1$ . Thus the wall location varies from 0 to  $L$  for a lattice of  $L$  sites. On a finite system of size  $L$  the domain wall performs a random walk in a lattice with reflecting boundary conditions. Therefore the probability to find the domain wall at time  $t$  and position  $i$  can be evaluated from:

$$\frac{dP(i, t)}{dt} = D_+ P(i - 1, t) + D_- P(i + 1, t) - (D_+ + D_-) P(i, t), \quad (4)$$

for  $1 \leq i \leq (L - 1)$ . At the (reflecting) boundaries one has

$$\frac{dP(0, t)}{dt} = D_- P(1, t) - D_+ P(0, t) \quad (5)$$

$$\frac{dP(L, t)}{dt} = D_+ P(L - 1, t) - D_- P(L, t), \quad (6)$$

where  $D_+ = \frac{\beta(1-\beta)}{1-\alpha-\beta}$  and  $D_- = \frac{\alpha(1-\alpha)}{1-\alpha-\beta}$ .

The stationary solution of Eqs. (4)–(6) in the low density phase  $\alpha < \beta$ ,  $\beta \leq 0.5$  is given by  $P(i) = \exp(-(L - x)/\xi)/\mathcal{N}$ , where the localization length is given by  $\xi = \log(D_+/D_-)$  and the normalization  $\mathcal{N}$  by  $\mathcal{N} = (1 - \exp(-(L + 1)/\xi))/(1 - \exp(-1/\xi))$ . In the high density phase one obtains analogous results by using the particle hole symmetry of the TASEP.

By using choice (3) for the hopping rates, one recovers the exact result for the localization length  $\xi$ .

### 3. PARTICLE NUMBER FLUCTUATIONS IN THE DOMAIN WALL PICTURE

The fluctuations of the number of particles  $N = \sum_i \tau_i$  are defined as:

$$\begin{aligned} \frac{\langle \Delta N \rangle}{L} &= \frac{\langle N^2 \rangle - \langle N \rangle^2}{L} \\ &= \frac{1}{L} \left[ 2 \sum_{i < j} \langle \tau_i \tau_j \rangle + \langle N \rangle - \langle N \rangle^2 \right], \end{aligned} \quad (7)$$

where the brackets  $\langle \dots \rangle$  denote an average over the stationary ensemble. Equation (7) illustrates the connection between the fluctuations and the two-point correlation functions. The fluctuations of the particle number, as well as the complete large deviation function, can be calculated using the exact stationary solution of the TASEP.<sup>(16)</sup> We show now, as a sensitive test of the accuracy of the DW theory for finite systems, how the results of the domain wall theory compare to the simulation results.

#### 3.1. Particle Number Fluctuations and the Domain Wall Theory

We now proceed to calculate the relevant quantities in the framework of the DW theory. The first quantity one has to calculate is the average number of particles. In the low density phase the stationary probability to find the shock at link  $i$  is given by  $P(i) = (1/\mathcal{N}) \exp(-(L-i)/\xi)$ . In the domain wall picture this means that one finds  $(L-i) \rho_+ + i \rho_-$  particles in the systems. So by summing over all possible shock positions one gets

$$\begin{aligned} \langle N \rangle &= \frac{1}{\mathcal{N}} \sum_{i=0}^L e^{-(L-i)/\xi} [(L-i) \rho_+ + i \rho_-] \\ &= \rho_- L + \frac{\delta e^{-1/\xi} (1 - (L+1) e^{-L/\xi} + L e^{-(L+1)/\xi})}{(1 - e^{-1/\xi})(1 - e^{-(L+1)/\xi})}, \end{aligned} \quad (8)$$

where  $\delta = \rho_+ - \rho_-$  denotes the density difference between the high and low density domain which coexist.

Next we have to calculate the two point correlations  $\langle \tau_i \tau_j \rangle$  for  $i < j$ . This is done by averaging over the particle densities if the domain wall

is located left from site  $i$ , between  $i$  and  $j$ , and right from site  $j$ , i.e., one finds

$$\langle \tau_i \tau_j \rangle = \frac{\rho_-^2}{\mathcal{N}} \sum_{k=0}^{i-1} e^{-(L-k)/\xi} + \frac{\rho_- \rho_+}{\mathcal{N}} \sum_{k=i}^{j-1} e^{-(L-k)/\xi} + \frac{\rho_+^2}{\mathcal{N}} \sum_{k=j}^L e^{-(L-k)/\xi}. \quad (9)$$

Using Eqs. (7)–(9) we get the following result for the variance of the number of particles:

$$\begin{aligned} \frac{\langle \Delta N \rangle}{L} &= \rho_- (1 - \rho_-) + \frac{\delta}{L} \frac{(1 - 2\rho_-) e^{-1/\xi}}{1 - e^{-(L+1)/\xi}} \left( \frac{1 - e^{-L/\xi}}{1 - e^{-1/\xi}} - L e^{-L/\xi} \right) \\ &+ \frac{\delta^2 e^{-2/\xi} (1 - e^{-2L/\xi}) - 2e^{-(L+3)/\xi} (1 - e^{-L/\xi})}{(1 - e^{-1/\xi})^2 (1 - e^{-(L+1)/\xi})^2} \\ &- \delta^2 e^{-(L+1)/\xi} \frac{1 + e^{-(L+1)/\xi} + L}{(1 - e^{-(L+1)/\xi})^2}. \end{aligned} \quad (10)$$

The corresponding results in the high density phase can be obtained by applying the particle hole symmetry of the TASEP. On the coexistence line ( $\alpha = \beta$ ) the localization length diverges and the fluctuations are given by:

$$\frac{\langle \Delta N \rangle}{L} = \frac{\delta}{2} (1 - 2\rho_-) + (1 - \rho_-) \rho_- + \delta^2 \frac{(L-4)}{12}. \quad (11)$$

### 3.2. Comparison with Simulation Results

Figure 1 shows a comparison between the calculated values and simulation results for the particle number fluctuations. The results are for  $\beta = 0.25$  and different values of  $\alpha$  surrounding the first order transition at  $\alpha = 0.25$ . Our simulations start in the low density phase, cross the coexistence line and end up in the high density phase. The agreement between DW-theory and simulation results is excellent for larger system sizes. For small system sizes one observes small deviations from the simulation results, which are presumably due to the finite width of the shock. Nevertheless, we stress the fact that the DW theory gives correct results (i.e., within the accuracy of the simulations) already for systems of the order of hundred sites.

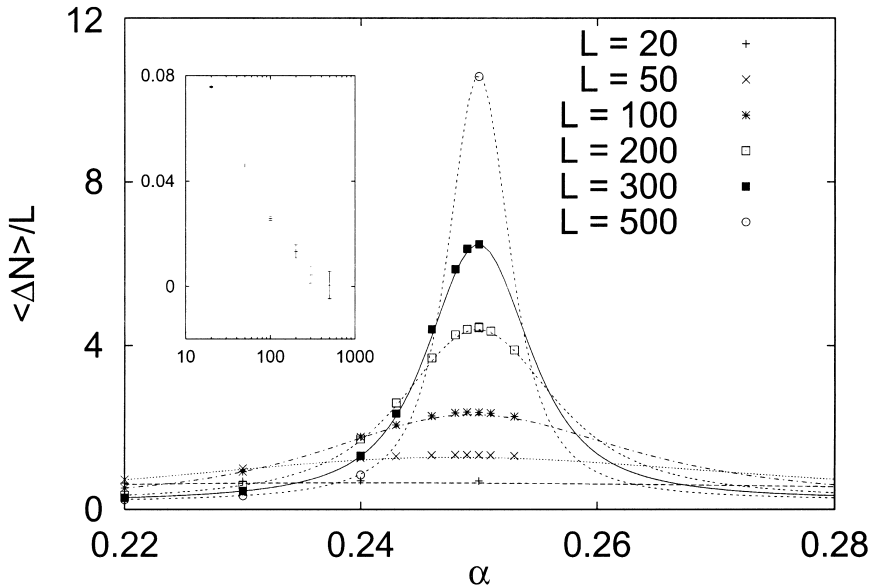


Fig. 1. Domain-wall prediction vs. simulation results of the particle number fluctuations  $\langle \Delta N \rangle / L$ . The symbols correspond to simulations results of the finite chain. The predictions of the domain wall picture are indicated by lines. We consider  $\beta = 0.25$  for all simulations. The inset shows the relative deviations  $(\langle \Delta N \rangle - \langle \Delta N \rangle_{DW}) / \langle \Delta N \rangle$  between simulations and domain-wall predictions. For  $L \geq 300$  the deviations are smaller than the numerical precision of our simulations.

### 4. NON-STATIONARY PROCESSES

The results for the stationary particle number fluctuations presented in the previous section—for which an exact solution exists—have provided a test for the accuracy of the domain-wall picture. But in contrast to the exact stationary solution the domain wall picture also allows to characterize the dynamics of the system in the transient regime.

#### 4.1. Density Profiles

In order to check the correctness of the phenomenological picture we investigated the time-dependent density profile interplaying between two stationary states. We started from a stationary state in the low density regime on the line  $\alpha_0 + \beta_0 = 1$ . Indeed, on this line, the exact stationary solution has a simple product form, and the density profile is flat.<sup>(10)</sup> This choice was made in order to keep the calculations simple, and to generate easily a large number of independent configurations. Suddenly, we change the output rate  $\beta$  such as to (i) lie on the coexistence line  $\beta = \alpha = \alpha_0$  or (ii)

cross the transition line into the high density phase so that  $\beta < \alpha = \alpha_0$ . We take as the origin of time the moment when this change occurs. A large number of independent simulations are performed in parallel. At regular time intervals, an ensemble average of the density profile over the independent simulations is performed. After some time, a new stationary state is reached.

In our simulations, we chose as initial condition  $\alpha_0 = 0.25$ ,  $\beta_0 = 0.75$ . At  $t = 0$ ,  $\alpha = \alpha_0$  stays fixed, while  $\beta$  is varied to (i)  $\beta = 0.25$ , or (ii)  $\beta = 0.2, 0.1$ , or  $0.02$ . This change is instantaneous. The density profile is averaged every 100 time steps over 100,000 independent simulations, i.e., we took 100,000 arbitrary configurations from the initial stationary ensemble and performed a simulation run for each initial configuration.

In the remaining part of this section we want to explain how this setup can be described by means of the domain wall theory.

The chosen set of parameters ensures the absence of a shock in the initial condition. By changing the right reservoir we introduced a shock at position  $L$  and time  $t = 0$ . In the course of time the motion of the wall then follows a random walk described by Eqs. (4)–(6).

In case (i) the random walk is symmetric, because  $\alpha = \beta$  and thus  $D_+ = D_-$ . An exact analytic solution for a random walk between two reflecting walls, starting at  $r=0$ , is known for all times:<sup>(17)</sup>

$$P(i, t) = \frac{1}{L+1} \left\{ 1 + \sum_{n=1}^{L+1} \exp \left( -2Dt \left\{ 1 - \cos \left[ \frac{\pi n}{L+1} \right] \right\} \right) \times \left[ \cos \left( \frac{i\pi n}{L+1} \right) + \cos \left( \frac{(i+1)\pi n}{L+1} \right) \right] \right\}. \quad (12)$$

At long times, the wall has a uniform probability to be located anywhere in the system.

In case (ii),  $D_+$  and  $D_-$  are different. The exact analytical solution of the asymmetric random walk with reflecting boundaries is also known,<sup>(15, 17)</sup> but for convenience we treated directly the discretized diffusion equation

$$P(i, t + dt) = D_+ dt P(i-1, t) + D_- dt P(i+1, t) + [1 - (D_+ + D_-) dt] P(i, t), \quad (13)$$

with equivalent expressions for the boundaries. We took  $dt$  small enough so that the results do not depend on the chosen value.

Once the distribution  $P(i, t)$  is known, the density profile can be computed for any time

$$\rho(i, t) = \left( \sum_{n=0}^i P(n, t) \right) \rho_- + \left( \sum_{n=i+1}^L P(n, t) \right) \rho_+ \quad (14)$$



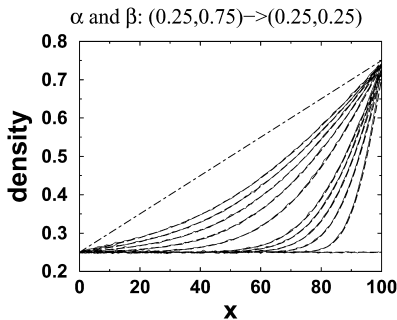


Fig. 2. Domain-wall prediction (dashed lines) vs. simulation results (solid lines) for the time dependent density profile when  $\beta$  is suddenly changed at  $t = 0$  from  $\beta = 0.75$  to  $0.25$ . The input rate is fixed  $\alpha = 0.25$  and the system size is  $L = 100$ . Each profile was averaged over 100000 independent simulations. The dot-dashed line indicates the asymptotic linear density profile.

where  $\rho_-$  and  $\rho_+$  are the effective densities of the left and right reservoirs, i.e.,  $\rho_- = \alpha$  and  $\rho_+ = 1 - \beta$  for the TASEP.

The comparison with the simulation results (see Figs. 2 and 3) shows an excellent agreement. In case (i), the domain wall undergoes a diffusive motion and the density profile modification scales as  $\sqrt{t}$ . To make the picture more clear, beyond  $t = 500$ , we show only the profiles every 500 time steps. In the long time limit, the domain wall is delocalized over the whole system and the density profile is linear.

In case (ii), the wall has a non vanishing drift velocity, and the shift of the density profile is linear in time, at least as long as boundaries are far enough. This is illustrated in Fig. 4 where the first density profiles (for  $100 \leq t \leq 500$ ) are translated by a multiple of 100 V. The averaged wall

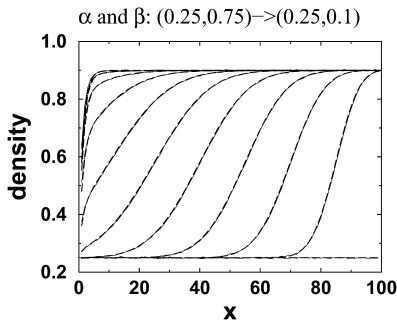


Fig. 3. Domain-wall prediction (dashed lines) vs. simulation results (solid lines) for the time dependent density profile when  $\beta$  is suddenly changed at  $t = 0$  from  $\beta = 0.75$  to  $0.1$ . The input rate is fixed  $\alpha = 0.25$ . Profiles are plotted every 100 time steps. Each profile was averaged over 100000 independent simulations. The system size is  $L = 100$ .

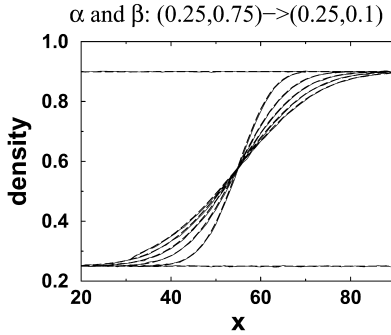


Fig. 4. Same figure as 3, but with the density profiles translated by a multiple of 100 V.

velocity  $V$  is given by Eq. (2). Of course, as the wall position distribution evolves from a Dirac function into a larger and larger gaussian, the density profile flattens as time increases. At long times, the wall is located near the left boundary, and the density profile is flat, apart from an exponential boundary layer at the entrance of the system (Fig. 3).

For small systems, the agreement between domain wall theory and simulations is not so good, as expected. However, even for a system of size  $L = 10$ , the domain wall results still indicate quite well the non-stationary behavior, as long as the wall is far enough from the left boundary (Fig. 5). Surprisingly, the agreement is much better at the beginning, when the wall is still near the right boundary. It could be linked to the fact that in the initial condition, as the density profile is flat, the domain wall approximation (with a wall on the right of the system) is exact.

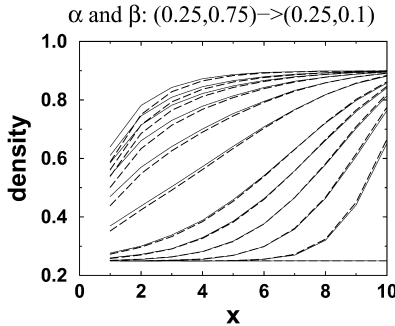


Fig. 5. Domain-wall prediction (dashed lines) vs. simulation results (solid lines) for the time dependent density profile when  $\beta$  is suddenly changed at  $t = 0$  from  $\beta = 0.75$  to 0.1. The input rate is fixed  $\alpha = 0.25$ . Profiles are plotted at time 0, 5, 10, 15, 20, 25, 28, 31, 34, 37, 40, and 500. Each profile was averaged over 100000 independent simulations. The system size is  $L = 10$ .

### 4.2. Fluctuations in the Particle Number

So far we focused on density profiles. Now we shall show that the domain wall picture allows also to predict the fluctuations in the total number of particles in a dynamical regime. From the calculation in the previous section, the time dependent probability distribution  $P(i, t)$  is known. The fluctuations are evaluated from formulas similar to (8)–(9), but now we replace the stationary distribution  $e^{-(L-i)/\xi}$  by  $P(i, t)$ . This yields

$$\langle N \rangle(t) = L\rho_- + (\rho_+ - \rho_-) \sum_{k=0}^L (L-k) P(k, t) \tag{15}$$

and

$$\langle \tau_i \tau_j \rangle(t) = \frac{\rho_-^2}{\mathcal{N}} \sum_{k=0}^{i-1} P(k, t) + \frac{\rho_- \rho_+}{\mathcal{N}} \sum_{k=i}^{j-1} P(k, t) + \frac{\rho_+^2}{\mathcal{N}} \sum_{k=j}^L P(k, t). \tag{16}$$

Using these expressions with the definition (7), the variance of the number of particles can be computed numerically for any time, and compared with the direct simulation results. Figure 6 presents such a comparison in case (ii), i.e., for a final value  $\beta = 0.1$ . Time has been divided by the average time needed for the wall to cross the system, i.e.,  $L/V$  where  $V$  is given by Eq. (2). The agreement is excellent for all sizes, though for  $L = 50$ , some small finite size effects are visible.

In the early linear stage, the wall has not yet reached the left boundary, and the curves superimpose for all sizes. When the wall arrives near the left boundary, the width of the probability distribution  $P(i, t)$  scales as  $\sqrt{L}$ . Thus the typical time during which domain walls reach the left boundary in the different realizations of the system also scales as  $\sqrt{L}$ . As

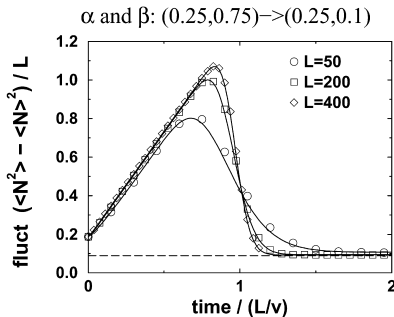


Fig. 6. Fluctuations in the total number of particles as a function of time (rescaled by  $L/V$ ). The simulations (symbols) are compared with the domain wall estimate (black continuous lines) with excellent agreement. The dashed line indicates the value  $\rho_+(1 - \rho_+) = 0.09$ .

time has been rescaled by  $L$  in Fig. 6, this transient separating the linear growth from the final stationary state tends to a sharp jump as  $L$  becomes large.

In the final stationary state, the fluctuations within the high density phase dominate. They can be estimated from the mean field expression  $\rho_+(1 - \rho_+) = (1 - \beta) \beta = 0.09$ .

## 5. CONCLUSIONS

Our results have shown that many features of the TASEP with open boundary conditions can be understood by analyzing the domain wall dynamics. For the stationary state, where the DW theory is known to give exact results in the limit of large  $L \rightarrow \infty$ ,<sup>(12)</sup> we calculated the fluctuations of the particle number for chains of various sizes. As being the integrated two-point correlation functions the fluctuations of the particle number are a sensitive test for the accuracy of the DW theory. We found that the predictions of the DW theory are numerically indistinguishable from the simulation results for  $L \gtrsim 100$ .

But beyond that we also found an excellent agreement in the transient regime. This is of particular interest, because the transient regime is out of scope of exact solution. The perfect agreement (up to the precision of our measurements) between simulation results and DW theory shows that the domain wall motion determines exclusively the relaxation processes, i.e., the coupling to the particle reservoirs is instantaneous. For future work it will be interesting to see whether other relaxation mechanisms are of importance if the domains are not of a simple product measure.

In several other studies it has been shown that the DW approach correctly predicts the phase diagram for a large number of models and update schemes.<sup>(14, 18, 19)</sup> In general cases, where an exact solution of the process is not possible, one has to establish the coupling to the chain and the flow density relations numerically. However, also in this case the domain wall interpretation is useful: First of all the parameter space is reduced drastically (e.g., the bulk density corresponding to a particular input prescription can be obtained from a *single* simulation run with free right boundary), and second it allows for a better characterization of the physical behavior.<sup>(14)</sup> Let us illustrate the latter point by the example of the Nagel–Schreckenberg model for traffic flow with maximal velocities  $v_{\max} > 1$ .<sup>(21)</sup> In this case one has several possibilities to implement the in- and output of the particles. This choice can produce even qualitatively different results for the phase diagram. E.g., it is necessary to apply a reservoir that can achieve the full capacity of the chain for a given model, in order to observe the maximum current phase (see ref. 20 for a counter-example). While for the TASEP the natural input of

particles on the first site of the chain fulfills this prerequisite, this is more subtle for particles which can move with higher velocities.<sup>(14)</sup> The difficulties in finding a suitable particle reservoir can be circumvented using the basic idea of the domain wall theory for the description of the particle reservoir. Instead of describing the capacity of the reservoirs in terms of in- and output probabilities we recommend to describe a particle reservoir by its effective density, i.e., by the bulk density which corresponds to a specific parameter combination, and to calculate the phase diagram only thereafter.

Summarizing, we have shown that the DW theory is able to reproduce the behavior of the TASEP with open boundary conditions to a large extent, and we have used it to obtain new results for non-stationary flows. We expect that our results can be generalized to a wide class of models for particle transport.

## ACKNOWLEDGMENTS

We acknowledge fruitful discussions with G. Schütz, B. Derrida, and A. Schadschneider. L.S. acknowledges support from the Deutsche Forschungsgemeinschaft under Grant SA864/1-2.

## REFERENCES

1. H. Spohn, *Large Scale Dynamics of Interacting Particles* (Springer, Berlin, 1991)
2. B. Schmittmann and R. K. P. Zia, *Phase Transitions and Critical Phenomena*, C. Domb and J. L. Lebowitz, eds. (Academic Press, New York, 1995), Vol. 17.
3. G. M. Schütz, *Phase Transitions and Critical Phenomena*, C. Domb and J. L. Lebowitz, eds. (Academic Press, New York, 2000), Vol. 19.
4. D. Chowdhury, L. Santen and A. Schadschneider, *Physics Reports* **329**:199 (2000).
5. J. T. MacDonald and J. H. Gibbs, *Biopolymers* **7**:707 (1969).
6. J. Krug, *Phys. Rev. Lett.* **67**:1882 (1991).
7. T. M. Liggett, *Trans. Amer. Math. Soc.* **179**:433 (1975).
8. B. Derrida, E. Domany, and D. Mukamel, *J. Statist. Phys.* **69**:667 (1992).
9. G. M. Schütz and E. Domany, *J. Statist. Phys.* **72**:277 (1993).
10. B. Derrida, M. R. Evans, V. Hakim, and V. Pasquier, *J. Phys. A* **26**:1493 (1993).
11. A. B. Kolomeisky, G. M. Schütz, E. B. Kolomeisky, and J. P. Straley, *J. Phys. A* **31**:6911 (1998).
12. V. Belitzky and G. M. Schütz, to be published.
13. V. Popkov and G. M. Schütz, *Europhys. Lett.* **48**:257 (1999).
14. V. Popkov, L. Santen, A. Schadschneider, and G. M. Schütz, *J. Phys. A* **34**:L45 (2001).
15. M. Dudzinski and G. M. Schütz, *J. Phys. A* **33**:8351 (2000).
16. B. Derrida, J. L. Lebowitz, and E. R. Speer, *Phys. Rev. Lett.* **87**:150601 (2001).
17. M. Schwartz and D. Poland, *J. Chem. Phys.* **63**:1 (1975).
18. C. Pigorsch and G. M. Schütz, *J. Phys. A* **33**:7919 (2000).
19. K. Klauk, Ph.D. thesis, Cologne (2000).
20. S. Cheybani, J. Kertesz, and M. Schreckenberg, *Phys. Rev. E* **63**:016108 (2001)
21. K. Nagel and M. Schreckenberg, *J. Physique I* **2**:2221 (1992).